SoftwareX 34 (2026) 102700

Contents lists available at ScienceDirect

SoftwareX

journal homepage: www.elsevier.com/locate/softx

Original software publication

Shimexpy: A python package for spatial harmonic imaging

Jorge Luis Beltran Diaz, Danays Kunka*

Institute of Microstructure Technology (IMT), Karlsruhe Institute of Technology (KIT), Hermann-von-Helmholtz-Platz 1, Eggenstein-Leopoldshafen, 76344, Baden-Württemberg, Germany

ARTICLE INFO

Keywords:
Spatial harmonic imaging
X-ray multicontrast
Mesh-based x-ray imaging
Python package

ABSTRACT

Spatial Harmonic Imaging (SHI) is a multicontrast and single-shot X-ray imaging modality that retrieves attenuation, differential phase, and scattering information from Fourier space. Although single-shot measurements are inherently fast, obtaining the three SHI contrasts in a fully processed form still requires a dedicated and efficient computational pipeline, particularly one that is cross-platform and integrable into user-defined workflows—capabilities that existing implementations do not currently provide. In this paper, we present `Shimexpy`, an open-source Python package that automates Fourier-domain processing, harmonic extraction, and the reconstruction of attenuation, differential phase, and scattering contrasts. The package provides a modular design and Python API, supports cross-platform environments, and promotes reproducibility through scripted pipelines and open licensing. We outline the software architecture, the core algorithms, open experimental datasets, and a minimal reproducible example. We additionally discuss performance, portability, and extensibility.

Metadata

Code metadata (mandatory)

Nr.	Code metadata description	Metadata
C1	Current code version	v0.1.0
C2	Permanent link to code/repository used for this code version	https://github.com/JLBeltran-IMAG/shimexpy
C3	Permanent link to Reproducible Capsule	Not available
C4	Legal Code License	Apache License 2.0
C5	Code versioning system used	git
C6	Software code languages, tools, and services used	Python
C7	Compilation requirements, operating environments & dependencies	Linux, Windows, macOS; NumPy, SciPy, xarray, Dask, scikit-image, matplotlib, tifffile, PySide6, CuPy
C8	If available Link to developer documentation/manual	Not available
C9	Support email for questions	jlbeltran930128@gmail.com

1. Motivation and significance

Since the first publication of *Spatial Harmonic Imaging* [1] (SHI, also referred to in the literature as *mesh-based X-ray imaging*), the technique has gradually matured into a robust single-shot approach capable of retrieving multicontrast images from a single exposure [1–8]. SHI achieves this by introducing a periodic modulator into the beam path and analyzing the resulting intensity modulation in Fourier space. Through harmonic decomposition, the zeroth-order component encodes the conventional attenuation signal, whereas the first-order harmonics encode phase and scattering information.

A key advantage of the single-shot spatial harmonic approach is the rapid data acquisition without phase-stepping procedures. This makes the method particularly suitable for dynamic experiments [9,10], and simplifies its integration into laboratory systems. Another important feature of the method is the possibility of implementing particle size selectivity [11,12]. By isolating specific harmonic components in the spatial

* Corresponding author.
Email address: danays.kunka@kit.edu (D. Kunka).

https://doi.org/10.1016/j.softx.2026.102700
Received 16 January 2026; Received in revised form 19 April 2026; Accepted 27 April 2026
Available online 11 May 2026

frequency domain, scattering contributions can be filtered according to characteristic length scales, enabling preferential sensitivity to structures above a defined threshold while suppressing background signals from smaller features [13]. Such selectivity opens up relevant application pathways in nanometric and micrometric particle tracking, targeted contrast-agent imaging, and functionalized particle-based therapies.

A known limitation of pure single-shot SHI implementations is that spatial resolution is constrained by the modulator period and by the spectral separation of harmonics in Fourier space. However, effective multi-stepping approaches have demonstrated that resolution can be significantly improved beyond Fourier harmonic operations, while partially preserving the advantages of rapid acquisition [14–17].

Despite its conceptual simplicity, the computational implementation of SHI remains nontrivial. Recently, a framework optimizing the complete SHI workflow, from data acquisition to post-processing, was introduced [18]. That study demonstrated the feasibility of implementing efficient, fast, and user-friendly workflows for Spatial Harmonic Imaging. Nevertheless, the framework remains restricted to Linux-based operating systems (specifically Ubuntu/Debian distributions) because of its dependence on `posixpath` and file-handling operations valid only for Unix-like environments. Although the system performs reliably and efficiently under Linux, this dependency constrains its applicability to dynamic studies and limits its adoption among users working on other platforms.

Apart from these portability constraints, the previous framework reported in [18], already implemented good software engineering practices, including modular routines for harmonic isolation, order labeling, phase retrieval, and contrast reconstruction—tasks often implemented through ad hoc or non-reproducible scripts [19]. Unfortunately, no other open-source software dedicated to Spatial Harmonic Imaging could be found in the literature or in public repositories, although related works in the broader field of multicontrast X-ray imaging remain highly promising and innovative.

Consequently, there is a clear need for dedicated, modular, and open-source software frameworks that not only implement the complete SHI workflow in a reproducible and portable manner [18], but also provide a truly independent cross-platform and operating system analysis environment, enabling seamless integration with other computational frameworks. To address this gap, we present `Shimexpy` (*Spatial Harmonic Imaging and MEsh-based X-ray Imaging Python package*), an open-source Python package that automates the full harmonic-domain analysis of SHI data. `Shimexpy` provides a unified, extensible and cross-platform environment, promoting reproducibility, accessibility, and ease of adoption in different research infrastructures.

1.1. Spatial harmonic and mesh-based x-ray imaging techniques

The experimental setup of Spatial Harmonic Imaging (SHI) is illustrated in Fig. 1. It consists of an X-ray source, a periodic optical element (such as a one-dimensional grating, a two-dimensional mesh, a checkerboard pattern, or an inverted Hartmann mask), the sample under study, and a detector. The periodic structure modulates the incident wavefront, which is subsequently distorted by the sample before reaching the detector. To retrieve the multicontrast information, two images are typically acquired: one of the periodic structure without the sample and another with the sample in place. From these measurements, absorption, differential phase, and scattering contrasts can be reconstructed, followed by optional post-processing steps for quantitative or morphological and structural analysis.

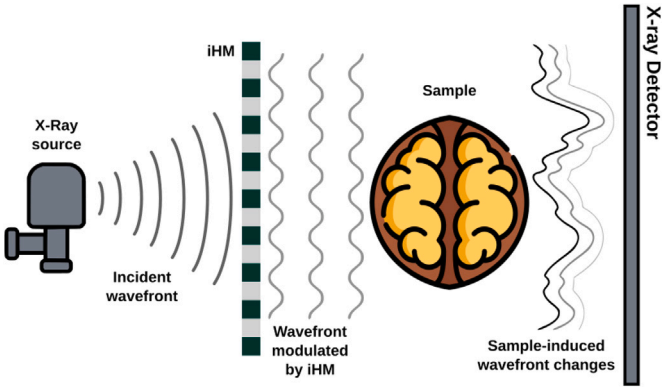

Fig. 1. Schematic experimental setup of spatial harmonic imaging (SHI).

1.2. Previous work

SHI-based experiments involve several stages, from data acquisition to final processing. Beltran et al. [18] addressed this complete workflow by providing a framework that covers all stages of the SHI modality. Lee et al. [20] demonstrated that Moiré and wraparound artifacts in differential phase images can be suppressed by rotating the mesh grid at an appropriate angle. Sun et al. [16] showed that combining mesh-grid shifting with wider windowing functions during Fourier processing improves spatial resolution while simultaneously reducing artifacts. Later, Lim et al. [21] demonstrated that applying a motion-blurring technique, i.e., translating the object rather than the mesh grid, can remove wraparound artifacts in scattering contrast images.

Despite these contributions, the computational landscape of SHI remains highly fragmented. Most available tools consist of ad hoc scripts, laboratory-specific routines, or platform-dependent pipelines, resulting in limited reproducibility, maintainability, and cross-platform usability [19]. Moreover, existing studies focus primarily on modifications of the experimental setup rather than on the processing stage, where SHI data processing remains insufficiently standardized and inconsistent across platforms. Beltran et al. provided a unified workflow implemented in open-source Python, but its strong reliance on POSIX directory structures limited portability to Debian/Ubuntu-based platforms, restricting broader adoption across Windows and macOS systems and complicating deployment in heterogeneous computational environments.

2. Software description

2.1. Modules of `Shimexpy`

The package `Shimexpy` is organized into five main modules (Fig. 2). Each module is independent and interacts with the others through a lightweight and consistent data interface. Internally, data are managed using labeled arrays, ensuring that the correct relationships between sample and reference datasets are preserved throughout the contrast-retrieval pipeline. The main modules are the following.

- `core` provides the principal routines for Fourier transform operations, harmonic extraction and labeling, phase demodulation and unwrapping, and normalization between sample and reference datasets.

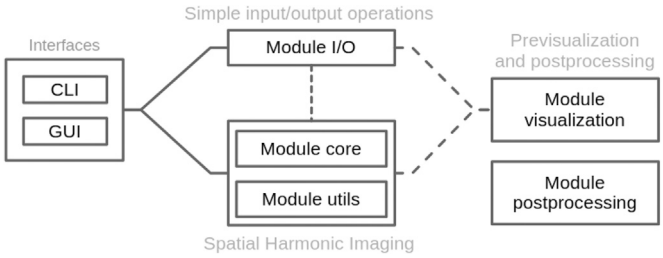

Fig. 2. Modules of `Shimexpy`. The `core` and `io` modules are required for all processing steps, while the remaining modules extend reconstruction, visualization, and postprocessing capabilities.

- `io` handles image import and export (TIFF, HDF5) together with basic metadata management.
- `utils` offers auxiliary routines, including an interactive region-of-interest (ROI) selection tool for defining the processing area.
- `visualization` includes Matplotlib-based plotting utilities for inspecting intermediate stages of the reconstruction and the final contrast images.
- `post` provides tools for pixel-wise comparison and quantitative analysis of reconstructed contrasts, enabling further interpretation of physical or morphological features.

In addition, `Shimexpy` includes a lightweight Graphical User Interface (GUI) and an extended Command-Line Interface (CLI), adapted from the public repository described in [18]. Both interfaces expose the complete SHI workflow and allow users to perform harmonic extraction and multicontrast reconstruction in either interactive or scripted environments.

2.2. Features of `Shimexpy`

2.2.1. Harmonic extraction and analysis

`Shimexpy` performs harmonic analysis after the optional preprocessing preliminary steps in SHI, namely flat-field correction to improve background uniformity and stability, and selection of a region of interest (ROI) to reduce computational load. Once the corrected sample and reference images are prepared, the intensity patterns $I(x, y)$ are transformed into the Fourier domain using an orthonormal two-dimensional discrete Fourier transform:

$$F(k_x, k_y) = \mathcal{F}\{I(x, y)\}. \tag{1}$$

The magnitude spectrum is

$$A(k_x, k_y) = |F(k_x, k_y)|. \tag{2}$$

Harmonic components are isolated through a deterministic, peak-centered strategy. The center of a harmonic is determined as the global maximum of the magnitude spectrum over the discrete Fourier domain

$$(k_{x0}, k_{y0}) = \arg\max_{(k_x,k_y)\in\Omega} A(k_x, k_y), \tag{3}$$

where Ω denotes the complete discrete Fourier domain.

In the original SHI formulation [1], harmonic windows are typically defined around theoretical spatial frequencies $\pm 2\pi/p$, implicitly assuming ideal periodicity and perfect alignment of the modulator. However, in practical implementations, small grid rotations, projection effects, and geometric misalignments may shift the spectral peaks away from their theoretical positions. For this reason, `Shimexpy` centers each harmonic window on the detected spectral maximum rather than on a predefined theoretical coordinate.

The size of the extraction window is defined in wavevector space through a spectral band-limit parameter k_{limit}. Let $k_x(j)$ and $k_y(i)$ denote the discrete frequency axes. The half-widths of the rectangular window are defined as

$$\Delta_y = \arg\min_i |k_y(i) - k_{\text{limit}}|, \tag{4}$$

$$\Delta_x = \arg\min_j |k_x(j) - k_{\text{limit}}|. \tag{5}$$

The harmonic extraction region is therefore defined as

$$\mathcal{R}_{m,n} = \left\{(k_x, k_y) \;\middle|\; |k_x - k_{x0}| < \Delta_x,\ |k_y - k_{y0}| < \Delta_y\right\}. \tag{6}$$

All Fourier coefficients within this region are assigned to the corresponding harmonic component. After extraction, the same region is set to zero in a working copy of the Fourier spectrum to prevent re-detection during iterative identification of higher-order harmonics.

The default value $k_{\text{limit}} = 0.5$ in Eqs. (4) and (5) (in units consistent with the discrete frequency axes) was selected to ensure reliable isolation of first-order harmonics under typical laboratory configurations while avoiding spectral overlap. Because the discrete Fourier transform samples spatial frequencies on a discrete grid, the theoretical harmonic frequencies are not guaranteed to coincide exactly with a discrete frequency bin. Consequently, the implementation selects the discrete frequency index whose value is numerically closest to the specified spectral band limit. This ensures consistency with the theoretical SHI formulation while respecting the discrete nature of the Fourier representation. The parameter remains fully configurable.

Each extracted harmonic block is subsequently transformed back to real space via the inverse Fourier transform, yielding complex-valued amplitude and phase maps. These harmonic components form the input for the subsequent reference-based normalization and multicontrast reconstruction stages.

2.2.2. Normalization

`Shimexpy` implements two complementary normalization stages: flat-field correction and reference-based normalization. Flat-field correction compensates for non-uniform illumination from the X-ray source and detector-related artifacts such as gain variations and defective pixels, ensuring that the subsequent harmonic analysis is not biased by instrumental inhomogeneities. In the reference-based normalization stage, the complex sample harmonics are divided by the corresponding reference harmonics. This operation corrects for stationary non-idealities of the periodic structure, yielding maps of attenuation, differential phase, and scattering contrasts. Both normalization steps are implemented in the `core` module, which provides low-level routines for stepwise processing as well as high-level convenience functions that execute the complete SHI normalization pipeline in a single call.

2.2.3. Processing workflow

A typical `Shimexpy` analysis follows the processing pipeline illustrated in Fig. 3. The workflow begins by loading the sample and reference images through the `io` module. Flat-field correction (FFC) is then applied to both datasets to compensate for illumination inhomogeneities and detector artifacts. Although applying FFC represents good experimental practice to improve background uniformity and stability, it is not an intrinsic computational requirement of the algorithm. An optional region-of-interest (ROI) cropping step may be performed to reduce computational load and restrict the analysis to the relevant field of view.

After preprocessing, the images are transformed into the Fourier domain, and spatial harmonics are extracted and labeled using the routines in `core`, as described in the previous subsection. For each extracted harmonic block, the inverse Fourier transform yields a complex spatial field $h_{m,n}(x, y)$.

The absorption contrast is computed as

$$\mu(x, y) = -\ln\left(\frac{|h^S_{00}(x, y)|}{|h^R_{00}(x, y)|}\right). \tag{7}$$

where the superscripts S and R denote the sample and reference images, respectively. For higher-order harmonics, normalized complex ratios are formed as

$$R^{S,R}_{m,n}(x, y) = \frac{h^{S,R}_{m,n}(x, y)}{h^{S,R}_{00}(x, y) + \varepsilon}, \tag{8}$$

where ε is a small regularization constant introduced to avoid numerical instabilities in regions of low intensity. The scattering contrast per harmonic is computed as

$$S_{m,n}(x, y) = -\ln\left(\frac{|R^S_{m,n}(x, y)|}{|R^R_{m,n}(x, y)|}\right), \tag{9}$$

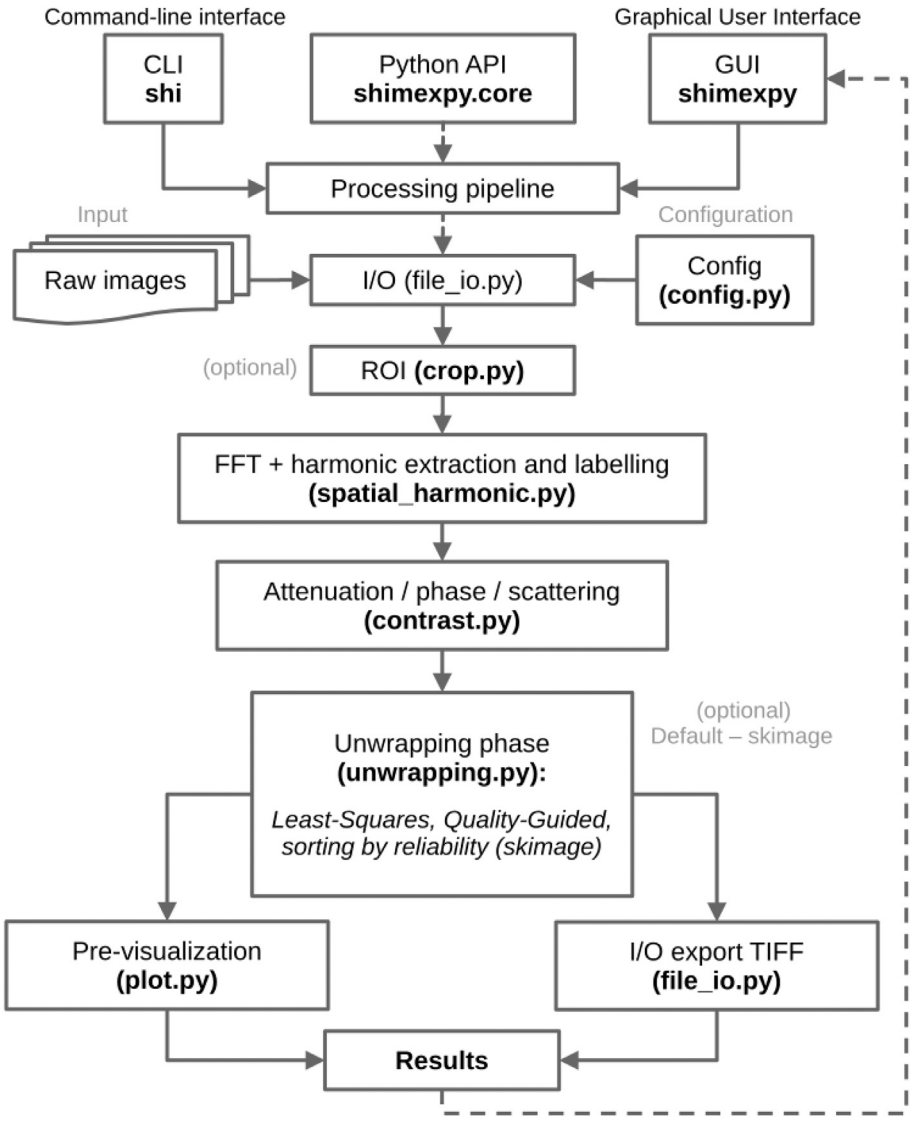

Fig. 3. Processing workflow implemented in `Shimexpy`. The pipeline includes image loading and configuration, flat-field correction, optional ROI selection, Fourier-domain harmonic extraction, reference-based normalization, optional phase unwrapping (default: quality-guided phase-unwrapping), and generation of the final multicontrast maps. Each stage can be executed interactively through the GUI, scripted through the CLI, or accessed programmatically via the Python API.

while the differential phase signal is obtained from

$$\phi_{m,n}(x,y) = \mathrm{unwrap}\Big[\arg R^{S}_{m,n}(x,y) - \arg R^{R}_{m,n}(x,y)\Big]. \tag{10}$$

Here, $\mathrm{unwrap}(\cdot)$ denotes a phase-unwrapping operator applied to remove discontinuities arising from the wrapped argument of the complex ratio.

The pseudocode corresponding to the workflow described above and illustrated in Fig. 3 is provided in the Supplementary Material for clarity and reproducibility. The only mandatory external parameter required to run the processing pipeline is the projected grid period. Other internal control parameters, such as the spectral band-limit used for harmonic windowing, the number of extracted harmonics, the regularization constant introduced for numerical stability, and the harmonic classification threshold, are assigned fixed default values in the current implementation. These parameters are documented in the public repository.

The reliability of the reconstruction is primarily governed by experimental conditions inherent to SHI acquisition rather than by algorithmic instability. Accurate harmonic isolation requires sufficient spectral separation and adequate signal-to-noise ratio in the Fourier magnitude spectrum. Additionally, the stability of the reference image directly influences the quantitative accuracy of the reconstructed contrasts. These constraints are intrinsic to SHI measurements and are not specific to the present implementation. In practice, incorrect projected period specification or insufficient fringe visibility may result in a degraded harmonic separation and reduced contrast fidelity.

2.2.4. *Differential phase retrieval*

In spatial harmonic imaging, differential phase contrast (DPC) is obtained from the argument of the first harmonic extracted in the Fourier domain from the measured image [3]. Since this quantity is computed through the complex argument operation, it is intrinsically wrapped in the interval $(-\pi, \pi]$ and may exhibit artificial discontinuities of amplitude $\pm\pi$. These discontinuities do not correspond to physical phase singularities but arise solely from the wrapped nature of the pseudo-phase field. Therefore, an additional spatial transformation is required to convert this wrapped pseudo-phase into a globally consistent DPC distribution.

To address this, Shimexpy incorporates two complementary unwrapping approaches that have been proven robust and reliable for SHI data. The first is the quality-guided phase-unwrapping algorithm implemented in scikit-image, which prioritizes locally reliable regions and propagates phase values based on pixel coherence. The second is a Poisson least-squares (LS-Poisson) unwrapping method [22], which computes a globally consistent solution by integrating wrapped gradients in the Fourier domain.

The availability of multiple unwrapping strategies allows users to select the method best suited to their imaging conditions, noise regime, and reconstruction goals. Quality-guided unwrapping [23] leverages local SNR variations to prioritize high-confidence regions, making it naturally compatible with the locally defined pseudo-phase fields produced by SHI. In contrast, LS-Poisson unwrapping [22] imposes global consistency without relying on the presence of phase residues, which aligns with the fact that SHI pseudo-phase fields typically exhibit wrapped jumps but lack topological singularities. Together, these approaches provide complementary tools for transforming wrapped harmonic-derived phase estimates into physically meaningful and quantitatively reliable DPC maps across a wide range of SHI scenarios.

Once unwrapped, the differential phase signal can be directly used in the final reconstruction stage of Shimexpy, or exported for downstream quantitative analysis.

2.2.5. Postprocessing workflow

In addition to the three reconstructed SHI contrasts, Shimexpy provides a dedicated postprocessing module for pairwise contrast analysis. This module generates pixel-wise dispersion plots in which each point corresponds to the attenuation–scattering (or any other two-contrast combination) values of a single spatial pixel. Such scatter–contrast representations were first used in the early SHI literature [1] to illustrate how multicontrast information can reveal structural differences not visible in attenuation alone.

The implementation in Shimexpy generalizes this idea into an interactive and reusable tool. Users can select a region of interest (ROI) and immediately obtain a two-dimensional contrast–contrast plot. The resulting visualization enables rapid assessment of material heterogeneity, microstructural variability, or clustering behavior directly from reconstructed SHI data, without requiring external analysis software.

This postprocessing tool is distributed as an auxiliary component within the Shimexpy suite and operates independently of the core reconstruction routines. It can be launched directly through the GUI or invoked as a standalone utility, providing a lightweight yet effective mechanism for downstream quantitative analysis. Although decoupled from the main processing pipeline, it complements the overall workflow by enabling fast contrast–contrast exploration without the need for external tools.

2.2.6. Performance and parallel execution

Although Shimexpy prioritizes portability and clarity over aggressive optimization, several components of the processing pipeline benefit from parallel execution. Internally, the package makes use of Dask-backed xarray operations, allowing Fourier transforms, harmonic extraction, and inverse transforms to be evaluated lazily and executed in parallel across available CPU cores. This enables efficient processing of multi-image datasets and reduces computation time without requiring users to manage multiprocessing constructs manually.

For GPU-equipped systems, Shimexpy optionally integrates CuPy as a transparent drop-in replacement for NumPy. When CuPy is available, selected array operations, including two-dimensional FFT through NVIDIA's cuFFT library, are executed on the GPU, while the same functions automatically fall back to standard NumPy implementations in CPU-only environments. This design preserves a consistent API and avoids mandatory CUDA dependencies while still enabling substantial acceleration for FFT-dominated workloads.

These performance features remain optional and unobtrusive: the full pipeline runs on standard CPU installations, whereas users with Dask or CUDA-enabled environments can benefit from additional parallelism and hardware acceleration without modifying their analysis scripts.

2.2.7. GUI, CLI and python API

Shimexpy provides three complementary interfaces: a graphical user interface (GUI), a command-line interface (CLI), and a Python API. All interfaces rely on the same core reconstruction engine, ensuring consistent numerical behavior across usage modes.

A lightweight cross-platform GUI is distributed with Shimexpy. The GUI allows users to load reference and sample images, define a region of interest (ROI), specify the projected modulator period, select the desired SHI contrast (absorption, scattering, or differential phase contrast), and compute and visualize the resulting reconstruction.

The GUI is deliberately minimal and serves primarily as a rapid inspection and demonstration environment for standard SHI workflows. Intermediate processing stages, such as harmonic peak detection, harmonic window configuration, order labeling, and normalization tuning, are not exposed in the current version. These steps are executed internally using fixed and reproducible routines.

For automated and large-scale processing, Shimexpy provides a command-line interface that exposes the main reconstruction routines. The CLI supports single-image analysis and batch processing of image folders, enabling integration into reproducible computational pipelines [18].

All internal routines, including FFT computation, harmonic extraction, reference normalization, and multicontrast reconstruction, are accessible through a documented Python API. This interface provides full parameter control and is intended for advanced users requiring customized processing strategies or integration into research pipelines.

A minimal usage example is shown in Listing 1.

2.2.8. Limitations/usage notes

Shimexpy implements the mathematical formalism of Spatial Harmonic Imaging. It does not perform hardware deconvolution. For experimental setups with extended X-ray sources or significant geometric blur where the point spread function (PSF) introduces severe spatial convolution, the spatial division of harmonics is insufficient to undo the physical blur. In such cases, users must apply an independent deblurring algorithm to the raw images before processing them through the Shimexpy pipeline to ensure quantitative accuracy.

3. Illustrative example

3.1. Experimental setup summary

The measurements presented in this work were performed using a laboratory cone-beam configuration. The X-ray source was a microfocus *Excillum MetalJet D2 +*, operated with an e-beam spot size of line focus $20\,\mu\text{m} \times 80\,\mu\text{m}$ and a nominal focal spot size $20\,\mu\text{m} \times 20\,\mu\text{m}$.

A periodic optical component, specifically an inverted Hartmann mask (iHM), was positioned in the incident beam. The iHM consists of electroplated gold pillars fabricated on a low-absorption substrate, with a period of $50\,\mu\text{m}$ and a pillar height exceeding $40\,\mu\text{m}$. The detector provided a full field of view of 5690×4608 pixels with a 16-bit dynamic range and a native pixel size of $49.5\,\mu\text{m}$. The exposure time was 2 seconds per projection. The geometric distances were as follows: 68 cm from the source to the modulator, 71 cm from the source to the sample, and 318 cm from the source to the detector.

The measured object was a test sample provided by Microworks GmbH.

Although the present manuscript focuses on computational analysis, a comprehensive description of the experimental acquisition framework is available in [18].

```
from shimexpy import load_image, ffc, get_all_contrasts

# Load test images
reference_img = load_image("../tests/example_data/flat_roi2.tif")
sample_img = load_image("../tests/example_data/smp_roi2.tif")
bright_img = load_image("../tests/example_data/bright_roi2.tif")
dark_img = load_image("../tests/example_data/dark_roi2.tif")

# Executing Flat-Field Correction (FFC)
ref_ffc = ffc(reference_img, dark_img, bright_img)
smp_ffc = ffc(sample_img, dark_img, bright_img)

period = 5 # projected period of modulator

# Calculating all contrast per channel
absorption, scattering, dpc = get_all_contrasts(smp_ffc, ref_ffc, period)
```

Listing 1. Minimal API example.

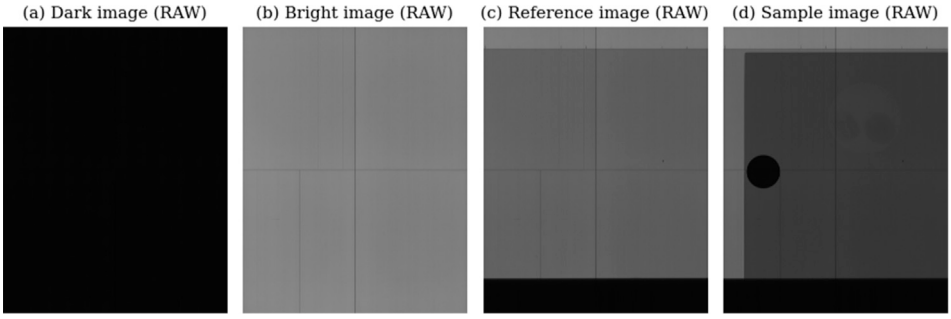

Fig. 4. Acquired images: (a) dark, (b) bright, (c) reference, and (d) sample frames. The sample consists of two corn seeds enclosed in a PMMA (polymethyl methacrylate) housing, followed by a printed label (Microworks) and a porous sponge layer.

3.2. SHI data processing with *Shimexpy*

To illustrate the usage and practical workflow of the Shimexpy package, we provide a representative example based on an experimental dataset acquired with the SHI configuration shown in Fig. 1. The example begins directly with real measurements, following the same processing pipeline shown in Fig. 3.

The acquisition produces four base images, shown in Fig. 4. Prior to Fourier-domain processing, it is often beneficial, although not strictly required, to crop the region of interest (ROI) and apply flat-field correction to suppress source and detector contributions.

After cropping, flat-field correction is applied using the corresponding dark and bright frames. This step removes detector offsets and illumination inhomogeneities, resulting in flat-field-corrected ROIs.

These two preprocessing steps, ROI selection and flat-field correction, are not strictly mandatory, but they are highly recommended for several reasons. First, selecting an appropriate region of interest significantly increases processing speed, which is particularly advantageous when SHI is used for real-time measurements or fast acquisition–processing workflows. By restricting the analysis to the region containing the relevant signal, unnecessary Fourier computations are avoided, and the overall reconstruction pipeline becomes more efficient.

Second, flat-field correction provides a direct assessment of the detector–source contributions. Shimexpy includes a dedicated tool to evaluate these effects. In the example shown here, flat-field correction produces only a modest reduction in global standard deviation, which is expected for a stable detector–source system dominated by photon statistics. However, the peak-to-peak intensity variation is reduced substantially (approximately 35%–47%), indicating that flat-fielding effectively removes large-scale illumination inhomogeneities, fixed-pattern variations, and residual gain differences.

The next step is the Fourier transform of the corrected data and harmonic extraction and labeling. Once the harmonic blocks are extracted and indexed for both the reference and the sample, contrast reconstruction can be performed. Fig. 5(a) shows the horizontal, vertical, and bidirectional scattering contrasts retrieved from the first-order harmonics. Similarly, Fig. 5(b) presents the differential phase contrast (DPC) reconstructed for the same three directional modes.

For most applications, the three primary contrasts (absorption, bidirectional scattering, and bidirectional differential phase) provide a complete multicontrast description of the object, as shown in Fig. 6. Alternatively, Shimexpy also exposes the full set of directional contrasts, useful for anisotropic samples or advanced analysis workflows.

Performance. On a standard workstation (Intel i7-class CPU, 32 GB RAM), processing a 2048×2048 SHI image requires approximately 0.3–0.6 s when using the CPU backend, and 0.05–0.1 s with optional GPU acceleration via CuPy. The exact runtime depends on the unwrapping strategy and the number of harmonics processed. Memory usage during reconstruction remains below 1 GB for images of this size. These values reflect typical experimental workloads and can be reproduced using the benchmarking scripts included with the package (Table 1).

4. Impact

The availability of Shimexpy influences the practical workflow of Spatial Harmonic Imaging experiments by reducing the technical overhead associated with data processing. By providing a compact Python package that exposes the complete SHI processing chain through a small

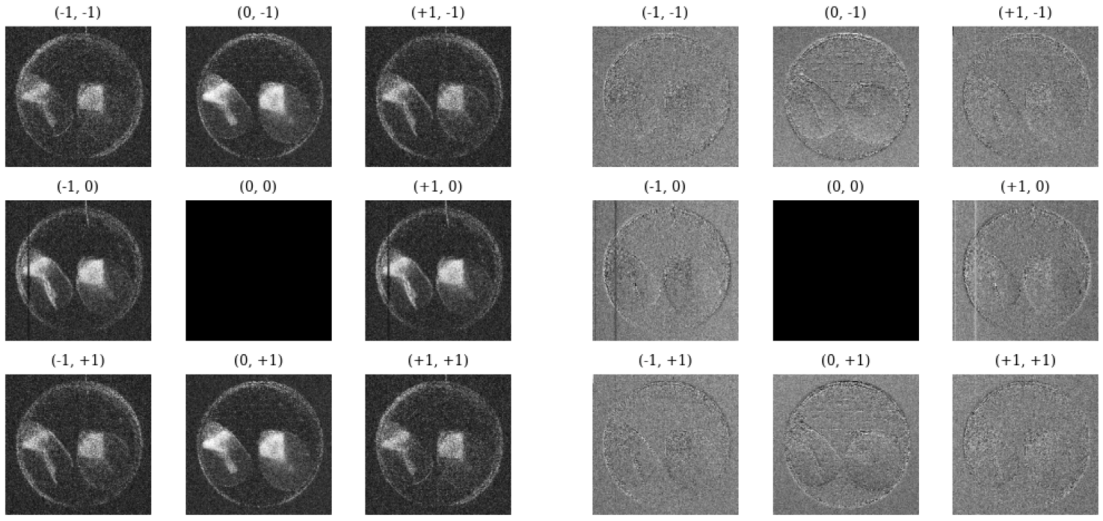

(a) Scattering contrast per harmonic component (b) DPC per harmonic component

Fig. 5. Contrast images obtained from Fourier components indexed by (m, n). (a) Amplitude-based scattering (dark-field) contrasts; (b) phase-based differential phase contrast (DPC) images. The phase unwrapping algorithm used to retrieve the DPC images was the quality-guided method implemented in `skimage.restoration.unwrap_phase`. The central $(0, 0)$ harmonic (DC term) is omitted, as it corresponds to attenuation contrast rather than phase or scattering information. The region of interest (ROI) was selected to encompass both corn seeds.

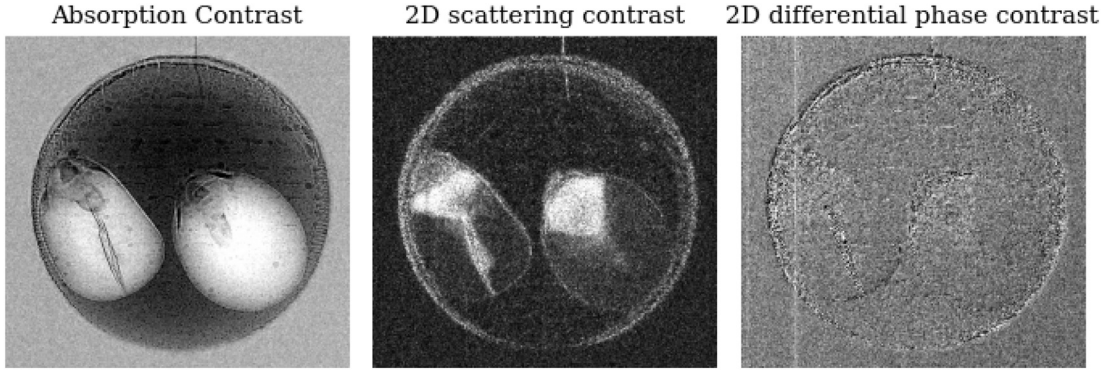

Fig. 6. Reconstructed absorption, 2D scattering, and 2D differential phase contrast (DPC) images. The 2D scattering and 2D DPC maps are obtained by combining the horizontal components reconstructed from the $(\pm 1, 0)$ harmonics and the vertical components reconstructed from the $(0, \pm 1)$ harmonics, using a normalized arithmetic average.

Table 1
Timing summary for the main stages of the `Shimexpy` pipeline. Times are reported for both reference and sample images.

Stage	Reference	Sample	Notes
FFT (auto-selection)	140.7 ms	10.66 ms	CuPy when available, otherwise NumPy
FFT (GPU)	10.34 ms	11.93 ms	Full GPU backend (cuFFT)
FFT (CPU)	62.99 ms	63.52 ms	NumPy `fft` implementation
Flat-field correction	0.012 ms	0.010 ms	CPU-only, negligible cost
Harmonic extraction	0.030 ms	0.025 ms	Parallelized via Dask

set of well-defined functions, the software allows researchers to allocate more effort to the investigation of contrast formation mechanisms and experimental design, rather than to the repeated implementation of processing pipelines.

In day-to-day research workflows, this abstraction simplifies Fourier-domain processing, harmonic extraction, normalization, and phase unwrapping, thereby enabling faster iteration during experimental campaigns. The possibility of computing SHI contrasts by supplying only the required input images through a stable and documented API represents a departure from earlier laboratory-specific scripts, in which processing logic was closely tied to particular experimental setups or operating systems.

The consistent interface of `Shimexpy` further supports the development of GPU-oriented extensions that follow the same processing logic as the CPU implementation. This design choice facilitates the transition from offline analysis to processing at the acquisition rate, providing real-time experimental feedback in dynamic and time-resolved SHI measurements without requiring changes to user code.

By adopting a permissive open-source license, the software supports reuse and extension within the X-ray imaging community and lowers barriers to integration into existing analysis environments. The inclusion of a fully reproducible and well-documented example provides a clear reference for new users and contributes to transparent and reproducible research practices.

`Shimexpy` is intentionally distributed as a Python package rather than as a monolithic framework. The accompanying command-line and

graphical interfaces are built directly on the same core functionality, extending usability across different user profiles while preserving a single, consistent implementation of the SHI processing pipeline.

5. Conclusions

`Shimexpy` offers a unified, open-source platform for SHI processing, enabling reproducible and portable workflows. By delivering a cross-platform, modular, and openly available implementation of the entire SHI processing pipeline, `Shimexpy` addresses the lack of standardized and reproducible software tools for harmonic-domain analysis in single-shot multicontrast X-ray imaging. The availability of a well-defined Python API, command-line tools, documented examples, and openly released experimental datasets supports the reuse, validation, and integration of `Shimexpy` into user-defined computational workflows and experimental pipelines.

The computational efficiency of the implemented pipeline further supports fast acquisition–processing workflows. Despite its current capabilities, several extensions remain for future development. Full GPU acceleration has been implemented in the repository and will be incorporated into upcoming documented releases to enable near real-time reconstruction during dynamic single-shot SHI measurements. While `Shimexpy` provides a modular foundation that can be extended toward multi-frame and multi-scanning modalities, full native support for these acquisition strategies is not yet implemented. Planned developments also include enhancements to the graphical interface, incorporating advanced preprocessing tools, stage-by-stage visualization of the processing pipeline, and interactive tuning of Fourier-domain window functions. In addition, further studies on scattering and phase contrast mechanisms will be conducted to deepen the physical understanding of these contrasts and to refine their computational implementation within the framework.

CRediT authorship contribution statement

Jorge Luis Beltran Diaz: Writing – review & editing, Writing – original draft, Visualization, Validation, Software, Project administration, Methodology, Investigation, Formal analysis, Data curation, Conceptualization. **Danays Kunka:** Writing – review & editing, Writing – original draft, Visualization, Validation, Supervision, Resources, Project administration, Methodology, Investigation, Formal analysis, Data curation, Conceptualization.

Declaration of generative AI and AI-assisted technologies in the writing process

During the preparation of this work the author(s) used ChatGPT (OpenAI), Writefull, and Grammarly in order to improve language quality, clarity, and overall text readability. After using these tools/services, the author(s) reviewed and edited the content as needed and take(s) full responsibility for the content of the published article.

Declaration of competing interest

The authors declare that they have no known competing financial interests or personal relationships that could have appeared to influence the work reported in this paper.

Acknowledgements

The authors acknowledge support from the Karlsruhe School of Optics and Photonics (KSOP) and the Ministry of Science, Research, and Arts of Baden-Württemberg as part of the sustainability financing of the projects of the Excellence Initiative II. We further acknowledge Microworks GmbH for providing the test object used in this study.

Appendix A. Supplementary data

Supplementary data to this article can be found online at doi:10.1016/j.softx.2026.102700.

References

[1] Wen H, Bennett EE, Hegedus M, Carroll S. Spatial harmonic imaging of x-ray scattering—initial results. IEEE Trans Med Imaging 2008. https://doi.org/10.1109/tmi.2007.912393
[2] Wen H, Bennett EE, Hegedus MM, Rapacchi S. Fourier x-ray scattering radiography yields bone structural information. Radiology 2009. https://doi.org/10.1148/radiol.2521081903
[3] Wen HH, Bennett EE, Kopace R, Stein A, Pai VM. Single-shot x-ray differential phase-contrast and diffraction imaging using two-dimensional transmission gratings. Opt Lett 2010. https://doi.org/10.1364/ol.35.001932
[4] Lim H, Lee H, Cho H, Seo C, Je U, Park C, Kim K, Kim G, Park S, Lee D, Kang S, Lee M. Investigation of image characteristics in phase-contrast X-Ray imaging (PCXI) using a conventional X-Ray grid. J Korean Phys Soc 2017;71(10):722–6. https://doi.org/10.3938/jkps.71.722
[5] Lee H, Jeon D, Lim H, Cho H, Park M, Youn W. Quantification of the effects of grid angulation on image quality in single-grid-based phase-contrast x-ray imaging. J Opt 2021;23(10):105605. https://doi.org/10.1088/2040-8986/ac2460
[6] Lim H, Cho H, Lee H, Jeon D. Quantification of dark-field effects in single-shot grid-based x-ray imaging. J Opt 2022;24(3):035608. https://doi.org/10.1088/2040-8986/ac3f93
[7] Allahyani WH, Pyakurel U, Redgate A, MacDonald CA, Petruccelli JC. Initial investigation of mesh-based x-ray phase tomography. In: Defense + commercial sensing; 2023. https://api.semanticscholar.org/CorpusID:260039974.
[8] Mikhaylov A, Beltran JL, Zakharova M, Vlnieska V, Münch D, Fohtung E, Pezzin S, Kunka D. Micro-reinforced polymer composite materials studied by correlative x-ray imaging. Nano Trends 2024. https://doi.org/10.1016/j.nwnano.2024.100035
[9] Zakharova M, Reich S, Mikhaylov A, Vlnieska V, dos Santos Rolo T, Plech A, Kunka D. Inverted hartmann mask for single-shot phase-contrast x-ray imaging of dynamic processes. Opt Lett 2019;44(9):2306–9. https://doi.org/10.1364/OL.44.002306. https://opg.optica.org/ol/abstract.cfm?URI=ol-44-9-2306.
[10] Zakharova M, Mikhaylov A, Vlnieska V, Kunka D. Single-Shot multicontrast x-ray imaging for in situ visualization of chemical reaction products. J Imaging 2021;7(11). https://doi.org/10.3390/jimaging7110221. https://www.mdpi.com/2313-433X/7/11/221.
[11] Lynch SK, Pai V, Auxier J, Stein AF, Bennett EE, Kemble CK, Xiao X, Lee W-K, Morgan NY, Wen HH. Interpretation of dark-field contrast and particle-size selectivity in grating interferometers. Appl Opt 2011;50(22):4310–9. https://doi.org/10.1364/AO.50.004310. https://opg.optica.org/ao/abstract.cfm?URI=ao-50-22-4310.
[12] Zakharova M, Mikhaylov A, Reich S, Plech A, Kunka D. Bulk morphology of porous materials at submicrometer scale studied by dark-field x-ray imaging with hartmann masks. Phys Rev B 2022;106:144204. https://doi.org/10.1103/PhysRevB.106.144204. https://link.aps.org/doi/10.1103/PhysRevB.106.144204.
[13] Stein AF, Ilavsky J, Kopace R, Bennett EE, Wen H. Selective imaging of nano-particle contrast agents by a single-shot x- ray diffraction technique. Opt Express 2010;18(12):13271–8. https://doi.org/10.1364/OE.18.013271. https://opg.optica.org/oe/abstract.cfm?URI=oe-18-12-13271.
[14] He C, Hayden D, MacDonald CA, Petruccelli JC. Computational resolution enhancement for mesh-based x-ray phase imaging. Commer Sci Sens Imaging 2018. https://doi.org/10.1117/12.2305097
[15] He C, Sun W, MacDonald CA, Petruccelli JC. The application of harmonic techniques to enhance resolution in mesh-based x-ray phase imaging. J Appl Phys 2019. https://doi.org/10.1063/1.5094167
[16] Sun W, He C, MacDonald CA, Petruccelli JC. Mesh-based and polycapillary optics-based x-ray phase imaging. Med Imaging 2019. https://doi.org/10.1117/12.2512628
[17] Sun W, MacDonald CA, Petruccelli JC. Propagation-based and mesh-based x-ray quantitative phase imaging with conventional sources. Comput. Imaging IV 2019. https://doi.org/10.1117/12.2520756
[18] Diaz JLB, Korvink JG, Kunka D. SHI: a framework for spatial harmonic imaging. Sci Rep 2026;16(1):4338. https://doi.org/10.1038/s41598-026-37029-5
[19] Reich S, Plech A. Shack-Hartman sensor wavefront reconstruction software. 56.03.20; LK 01 2018. https://doi.org/10.5445/IR/1000082060
[20] Lee H, Lim H, Jeon D, Park C, Lee D, Cho H, Seo C, Kim K, Kim G, Park S, Kang S, Park J, Kim W, Lim Y, Woo T. Eliminating artifacts in single-grid phase-contrast x-ray imaging for improving image quality. Comput Biol Med 2018;97:74–82. https://doi.org/10.1016/j.compbiomed.2018.04.013
[21] Lim H, Lee J, Lee S, Lee H, Cho H. Elimination of wraparound artifacts in spatial harmonic imaging using motion blurring. Opt Lasers Eng 2024;175:107999. https://doi.org/10.1016/j.optlaseng.2023.107999
[22] Ghiglia DC, Pritt MD. Two-Dimensional phase unwrapping: theory, algorithms, and software. Wiley, New York; 1998.
[23] Herráez MA, Burton DR, Lalor MJ, Gdeisat MA. Fast two-dimensional phase-unwrapping algorithm based on sorting by reliability following a noncontinuous path. Appl Opt 2002;41(35):7437–44. https://doi.org/10.1364/AO.41.007437